Pressure-driven phase transitions in TiOCl and the family (Ca, Sr, Ba)Fe_2As_2

2010 J. Phys.: Condens. Matter 22 164208

(http://iopscience.iop.org/0953-8984/22/16/164208)

IOP PUBLISHING JOURNAL OF PHYSICS: CONDENSED MATTER

J. Phys.: Condens. Matter **22** (2010) 164208 (7pp) doi:10.1088/0953-8984/22/16/164208

Pressure-driven phase transitions in TiOCl and the family (Ca, Sr, Ba)Fe_2As_2

Yu-Zhong Zhang, Ingo Opahle, Harald O Jeschke and Roser Valentí

Institut für Theoretische Physik, Goethe-Universität Frankfurt, Max-von-Laue-Strasse 1, 60438 Frankfurt am Main, Germany

E-mail: valenti@itp.uni-frankfurt.de

Received 30 June 2009
Published 30 March 2010
Online at stacks.iop.org/JPhysCM/22/164208

Abstract

Motivated by recent experimental measurements on pressure-driven phase transitions in Mott insulators as well as the new iron pnictide superconductors, we show that first principles Car–Parrinello molecular dynamics calculations are a powerful method to describe the microscopic origin of such transitions. We present results for (i) the pressure-induced insulator to metal phase transition in the prototypical Mott insulator TiOCl as well as (ii) the pressure-induced structural and magnetic phase transitions in the family of correlated metals AFe_2As_2 (A = Ca, Sr, Ba). Comparison of our predictions with existing experimental results yields very good agreement.

(Some figures in this article are in colour only in the electronic version)

1. Introduction

Understanding the microscopic origin of phase transitions in correlated systems is a challenging task both for theory and experiment due to the large number of degrees of freedom (electronic, lattice and orbital) involved in the transitions. In a Mott insulator a transition from an insulating to a metallic or even a superconducting state can be induced by doping the system with carriers, as in the case of the high-T_c cuprates [1], or by applying pressure, as in the κ-charge transfer salts [2, 3]. Pressure-driven Mott insulator to metal transitions have also been discussed in a few transition metal oxides such as MnO [4–6], V_2O_3 [7] and lately in TiOCl [8, 9]. Very recently, high-temperature superconductivity has been achieved in a new class of correlated metals, the iron pnictide compounds, both by doping as well as by setting the systems under pressure [10, 11]. The origin of this phase transition is still under strong debate.

External pressure-induced phase transitions are especially attractive for microscopic modeling since the chemistry of the system remains untouched, i.e. possible disorder as in the doping case is almost nonexistent, and one can concentrate on the lattice changes induced by pressure. A reliable microscopic description of such transitions requires a simultaneous treatment of the electronic and lattice degrees of freedom as is realized in the first principles Car–Parrinello molecular dynamics method [12]. Instead of considering the motion of the nuclei and the solution of the Kohn–Sham equation for the electrons at fixed atomic positions as separate problems, the Car–Parrinello method explicitly views the electronic states as dynamical variables and considers these as a unified problem. By writing a fictitious Lagrangian for the system which leads to coupled equations of motion for both ions and electrons, the lattice dynamics and electronic properties can be treated on the same footing. Furthermore, the Parrinello Rahman approach to molecular dynamics simulations at constant pressure [13] treats the lattice parameters as additional degrees of freedom, allowing the first principles observation of structural changes as a function of pressure. The great advantage of this procedure is the ability to deal in a straightforward manner with crystals with anisotropic compressibilities along different directions as in the case of TiOCl and the new iron pnictide superconductors. In the present work we will show by reviewing recent calculations on pressure-driven transitions in the multi-orbital Mott insulator TiOCl as well as the family of iron pnictides AFe_2As_2 (A = Ca, Sr, Ba) that the Car–Parrinello method is often more efficient than the more common Born–Oppenheimer methods for describing the features of the phase transitions.

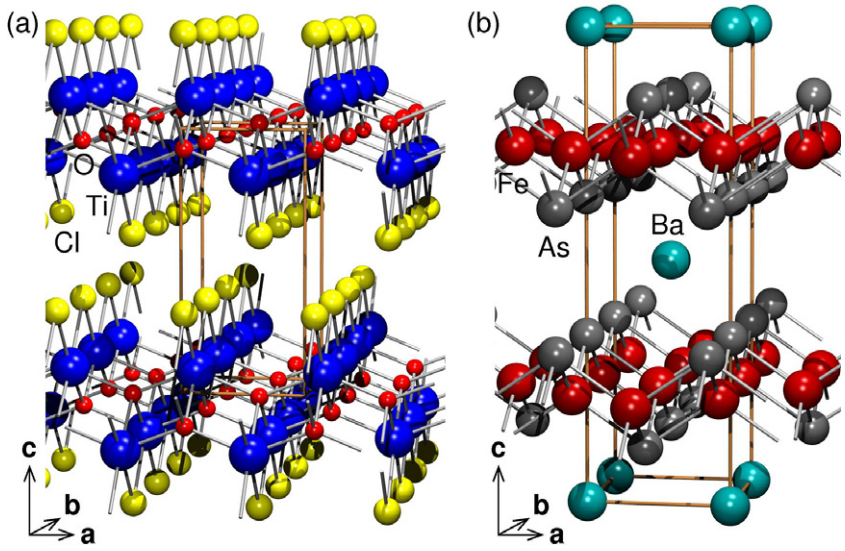

Figure 1. Lattice structures of (a) TiOCl and (b) AFe_2As_2 (A = Ca, Sr, Ba) for the example of $BaFe_2As_2$.

2. Overview of TiOCl and AFe_2As_2

TiOCl and AFe_2As_2 (A = Ca, Sr, Ba) are both layered compounds containing 3d transition metal ions as shown in figure 1. Correlation among the open d shell electrons is responsible for a rather unconventional behavior in these materials [8, 9, 11, 14–41]. In TiOCl, titanium (Ti) and oxygen (O) form bilayers stacked along the *c* direction and separated by chlorine (Cl) layers, while in AFe_2As_2 (A = Ca, Sr, Ba), layers of Fe–As tetrahedra are separated by alkaline earth metal ions.

2.1. TiOCl

TiOCl is a quasi-one-dimensional Mott insulator at room temperature where Ti chains along the *b* direction are weakly coupled [14, 15]. Upon lowering the temperature, TiOCl undergoes two consecutive phase transitions from a Mott insulating state to a spin-Peierls phase with dimerized Ti chains through an intermediate structural incommensurate phase with dominant out-of-chain incommensurability even under zero external magnetic field [16–19]. Since the discovery of this unusual intermediate phase, many efforts have been devoted to understand its microscopic origin [42–45]. Recently, a two-dimensional frustrated spin-Peierls model was proposed, where the model parameters were calculated from *ab initio* density functional theory (DFT) [42]. Besides the dominating interactions along chains, it was pointed out that the interchain magnetic frustrations may play an important role in the formation of the unconventional incommensurate phase in addition to the interchain elastic couplings.

Due to the $3d^1$ configuration of Ti^{3+} and quenching of the orbital degrees of freedom [18, 46], TiOCl was thought to be a model system for the one-band Hubbard model. In order to investigate a possible Mott insulator-to-metal transition in this system in the framework of the one-band Hubbard model, various experimental groups have recently investigated the effect of pressure [8, 9, 22–24] and electron doping [20, 21] on TiOCl. Interestingly, pressure-driven experiments lead to different conclusions. Kuntscher *et al* [8, 24] reported from optical measurements and x-ray diffraction analysis the observation of an insulator-to-metal transition at 16 GPa accompanied by a structural symmetry change. Forthaus *et al* [9], on the other hand, neither observed any indication of a metallic state up to pressures of 24 GPa from transport measurements nor did they identify from x-ray diffraction analysis changes on the crystal symmetry at 16 GPa. Recently, Blanco–Canosa *et al* [23] found a dimerized insulating state at high pressure by x-ray diffraction analysis and magnetization measurements combined with *ab initio* DFT results. The DFT calculations in [23] consisted in performing a structural optimization within the generalized gradient approximation (GGA) and an analysis of the electronic properties within GGA+U. It should be stressed that GGA gives a metallic state for TiOCl while GGA + U describes TiOCl as an insulator. In the following, we will argue that inclusion of strong correlation is crucial for obtaining the correct optimized lattice structure. Therefore, the theoretical understanding of the dimerization under pressure [23] may be questionable due to the alternate use of different functionals in one study.

In a recent work [22], we resolved the previous inconsistencies by performing *ab initio* Car–Parrinello molecular dynamics [12, 13] within the projector-augmented wave basis (CP-PAW) [47] on TiOCl under pressure. The GGA + U functional was considered throughout the whole study. Here $U = 1.65$ eV is used in order to reproduce the correct spin exchanges and therefore the high-temperature susceptibility behavior [14]. Within GGA + U correlation effects are included at the mean-field level. The simulations show that two phase transitions occur; a first one from the Mott insulating state to an intermediate dimerized metallic state accompanied by a symmetry lowering from orthorhombic $Pmmn$ to monoclinic $P2_1/m$, and a second transition to a normal metal with recovered $Pmmn$ symmetry. The first phase

transition is consistent with the observations of Kuntscher *et al* [8, 24] and the structural phase transition is in agreement with the experimental result of [23]. The second phase transition has not yet been reported experimentally. Moreover, the pressure effects involve the three t_{2g} orbitals in TiOCl.

2.2. AFe_2As_2

The materials AFe_2As_2 (A = Ca, Sr, Ba) are paramagnetic metals at room temperature. With decreasing temperature, a magnetic phase transition to a stripe-type antiferromagnetic (AF) ordered state and a structural phase transition from tetragonal to orthorhombic symmetry take place simultaneously [25–28]. Even more exciting is the fact that these systems are superconductors both under pressure [11, 36–40] and electron or hole doping [30–33], which has attracted considerable and persisting interest.

Since doping usually induces disorder, it is more practical to investigate the origin of the phase transition and the phenomenon of superconductivity by applying external pressure. However, while the pressure-driven magnetic and structural phase transitions in $CaFe_2As_2$ have been thoroughly investigated [34, 35], those in $SrFe_2As_2$ and $BaFe_2As_2$ have not yet been fully studied. Therefore, a theoretical prediction of the phase transitions in $SrFe_2As_2$ and $BaFe_2As_2$ is desirable since it is free of the Sn-problem. Unfortunately, it is well known that the magnetization and the volume of the iron pnictide compounds are overestimated by DFT calculations within GGA when structural optimizations are performed [48–50]. We will show here that due to this overestimation we only have to simulate higher pressures than the experimental ones in order to reach the experimental volume conditions while structural changes at critical pressures and the main features of the electron properties within different phases can still be captured properly.

Optimization of cell parameters and atomic positions under pressure within the framework of DFT has been done by Yildirim [51] and Xie *et al* [52]. By considering Vanderbilt-type ultrasoft pseudopotentials, a smooth structural transition for $CaFe_2As_2$ was observed under pressure without detection of a sudden sizable increase of the cell parameters a and b or a strong decrease of the cell parameter c which is inconsistent with experimental results [34]. Xie *et al* [52] optimized within the full potential linearized augmented plane wave method (FPLAPW) the orthorhombic lattice structure for $BaFe_2As_2$ under pressure by relaxing the internal parameter z_{As} and the c/a ratio while keeping the b/a ratio fixed. This procedure does not allow for the detection of the structural and magnetic phase transitions.

We investigated the phase transitions of AFe_2As_2 (A = Ca, Sr, Ba) under pressure in the lower-temperature region with the CP-PAW method within the spin-polarized GGA functional. The first-order phase transition from an orthorhombic phase to a collapsed tetragonal phase in $CaFe_2As_2$ is confirmed with relative changes of lattice parameters, bond lengths and angles agreeing very well with the experimental observations, indicating the validity of the application of the CP-PAW method to this system. At the critical pressure, an abrupt disappearance of magnetization is also found as observed experimentally. In particular, our calculations can account for the sudden expansion in the ab plane observed experimentally [34] at elevated pressure crossing the critical pressure as we discussed in [49], which was not obtained in other calculations. Applying this method to study $SrFe_2As_2$ and $BaFe_2As_2$, where less is known about the features of the phase transition, a simultaneous structural (orthorhombic to tetragonal) and magnetic phase transition is predicted at high pressure. However, we observe a weak first-order phase transition for $SrFe_2As_2$ and a continuous phase transition for $BaFe_2As_2$ in contrast to the strongly first-order phase transition in $CaFe_2As_2$. Finally, it should be pointed out that multi-orbital physics is important in AFe_2As_2 (A = Ca, Sr, Ba) since all five d orbitals cross the Fermi level.

3. Details of our calculations

In our studies of both systems, full, unbiased relaxations of all lattice and electronic degrees of freedom have been performed at each pressure value. In TiOCl, local coordinates are chosen as $x = b$, $y = c$, $z = a$ while in AFe_2As_2 (A = Ca, Sr, Ba), $x = a$, $y = b$, $z = c$.

All our calculations were performed with time steps of 0.12 fs at zero temperature. The system size was $4 \times 4 \times 4$ k points for AFe_2As_2 (A = Ca, Sr, Ba) and $6 \times 6 \times 6$ for TiOCl on doubled unit cells corresponding to different AF configurations [22, 49]. We used high energy cutoffs of 612 eV and 2448 eV for the wavefunctions and charge density expansion, respectively. The total energies were converged to less than 0.01 meV/atom and the cell parameters to less than 0.0005 Å. In TiOCl, a value of $U = 1.65$ eV was used for the GGA + U calculations with which correct spin exchange along b is reproduced [42]. In AFe_2As_2 (A = Ca, Sr, Ba), the 3s3p3d (4s4p4d/5s5p5d) states in Ca (Sr/Ba) are treated as valence states and 3d4s4p in Fe and As, while in TiOCl, the 3s3p3d4s in Ti, 2s2p in O and 3s3p in Cl are treated as valence states. We have checked our calculations within GGA based on these choices of valence states with the FPLAPW method as implemented in the WIEN2k code [53]. Very good agreement was found between these two methods, indicating the correctness of our constructed PAW basis for both systems. In figure 2, we show one of the comparisons for TiOCl between CP-PAW and FPLAPW within GGA. It is found that the total density of states (DOS) and partial DOS (pDOS) calculated from FPLAPW can be reproduced by CP-PAW. Not only the peak position but also the shape of the DOS are almost the same throughout the whole energy range. More spikes in the DOS from CP-PAW come from fewer k points used in the calculation.

Now let us investigate the effect of strong correlations on the lattice optimization [54] of TiOCl. In table 1, we present the optimized lattice parameters within different functionals compared to the experimental equilibrium state in TiOCl. For the lattice parameter c, we find that it is rather hard to determine precisely due to the fact that there only exist weak van der Waals forces between layers along c. Thus, by varying the lattice parameter c, the total energy remains almost

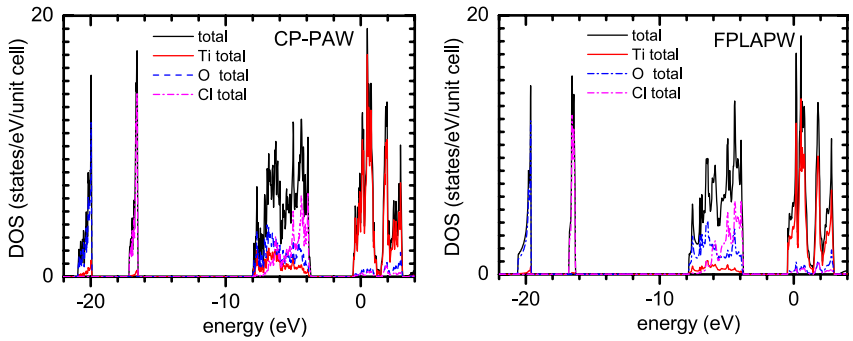

Figure 2. Comparison of the density of states for TiOCl obtained using the PAW (left panel) and the FPLAPW basis (right panel) methods within GGA. The agreement between the results obtained by both methods is very good and confirms the suitability of the PAW basis for TiOCl.

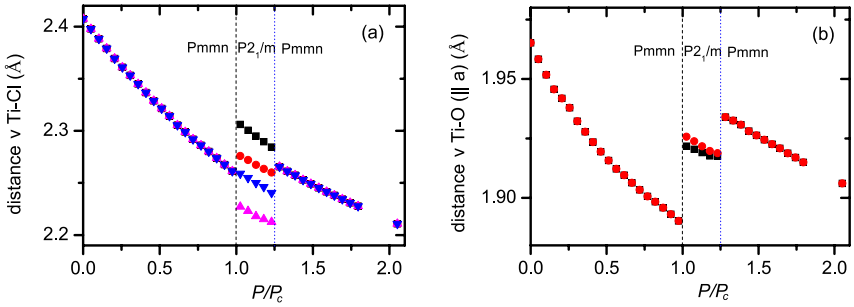

Figure 3. Calculated change of atomic distances of TiOCl as a function of applied external pressure, normalized to the critical pressure. (a) The distance between Ti and Cl. (b) The distance between Ti and O along a.

Table 1. Comparison of equilibrium lattice parameters for TiOCl optimized by different functionals. B3LYP data were obtained from [45].

	a (Å)	b (Å)	c (Å)
Exp.	3.79	3.38	8.03
CRYSTAL B3LYP	3.81	3.49	8.69
GGA	3.89	3.30	8.06
GGA + U (1.65, FM)	3.80	3.49	8.12
GGA + U (1.65, AF)	3.81	3.42	7.51

Table 2. Comparison of equilibrium atomic distances and angles for TiOCl optimized by different functionals. B3LYP data were obtained from [45].

	Ti–O$\|_a$ (Å)	Ti–Cl (Å)	Ti–O–Ti$\|_a$ (deg)
Exp.	1.96	2.40	150
CRYSTAL B3LYP	1.98	2.45	148.6
GGA	1.98	2.48	156.4
GGA + U (1.65, FM)	1.97	2.44	149.1
GGA + U (1.65, AF)	1.97	2.41	151.4

unchanged. For the lattice parameters a and b, B3LYP and GGA + U with both FM and AF configurations can provide a better comparison to experiment than GGA does, indicating the importance of strong correlations which are absent in GGA. Furthermore, it is found that the results from GGA + U with an underlying AF ordering are even better than those from GGA + U with FM ordering, which indicates that the correct setting of the spin configuration improves the lattice optimization. In table 2, we show the optimized atomic distances and angles by different functionals compared to the experimental results. Again, the same trend is found as in table 1, i.e. with the inclusion of correlations as implemented in GGA + U and in B3LYP, the optimized structures are closer to the experimental one.

In contrast to TiOCl, the iron pnictide compounds are metallic even in the AF state and are considered as moderately correlated systems. Therefore, the lattice optimizations for AFe_2As_2 (A = Ca, Sr, Ba) have been performed within GGA.

4. Results

4.1. TiOCl under pressure

In the study of TiOCl under pressure, we use a renormalized pressure due to the overestimation of the critical value. However, it has a different origin compared to that in AFe_2As_2 (A = Ca, Sr, Ba). As reported from experiments [15], TiOCl is a Mott insulator at room temperature and ambient pressure. Only short-range AF spin fluctuations exist in TiOCl. However, to reach the insulating state by DFT calculations, one has to impose certain long-range spin ordering. It is well known [55] that the AF insulator is more robust than the paramagnetic Mott insulator under bandwidth control; one has to apply much higher pressure to induce an insulator-to-metal transition if long-range AF ordering is present.

In figure 3 we present the calculated change of atomic distances as a function of applied external pressure. The lattice

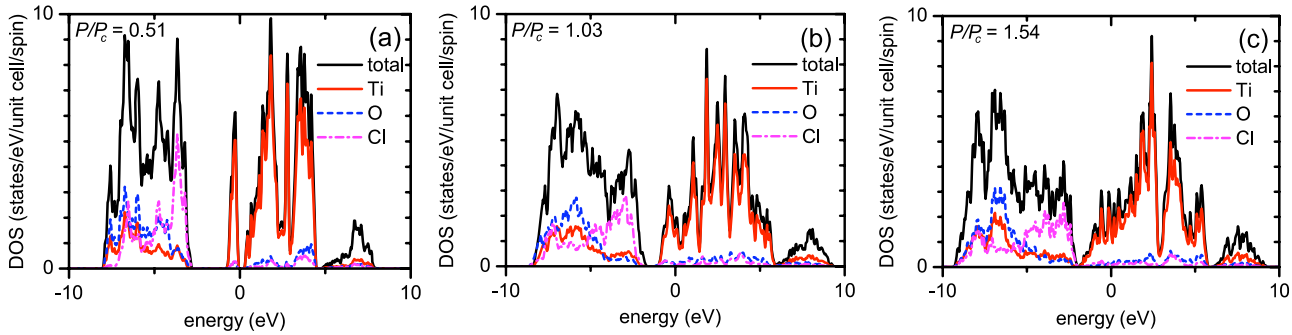

Figure 4. Density of states of TiOCl in three different phases. (a) is for the low pressure Mott insulating state ($P < P_c$), (b) for the dimerized metallic phase ($P_c < P < P_c'$), (c) for the uniform metal ($P > P_c'$).

parameters at each pressure are obtained by fully relaxing the lattice structure without any symmetry constraints. Although a magnetic ordering has to be imposed within the GGA + U functional (AF ordering along b and FM configuration along the other directions) the results are completely consistent with the experiments [9, 24].

At $P = P_c$ (black dashed vertical line in figure 3), the equivalent Ti–Cl distances in the lower pressure region split into four different values (see left panel) and the Ti–O distance into two (see right panel), indicating a lowering of the symmetry. We found that the space group changes from $Pmmn$ to $P2_1/m$ which agrees with the experimental observation [23]. Most interestingly, both non-equivalent Ti–O distances show jumps at this phase transition, indicating that the system expands along a in agreement with experiment [56]. Further increasing the external pressure, we find a second jump of the atomic distances at $P = P_c' > P_c$ (blue dotted vertical line in figure 3). At this pressure, all the non-equivalent Ti–Cl and Ti–O distances become equivalent again, indicating the recovery of the $Pmmn$ symmetry. The existence of this phase transition is currently under experimental investigation.

Figure 4 presents the DOS in these three phases. Figure 4(a) shows the DOS for the lower pressure case. The DOS looks very similar to that at ambient pressure except for the widening of the bands and the reduction of the gap amplitude. Right above the first phase transition, the gap is closed as shown in figure 4(b), which means that the system should show metallicity. The obtained insulator-to-metal transition is consistent with optical experiments [8, 24] but contradicts the electrical resistivity measurements [9]. A possible reason is that TiOCl is a strongly anisotropic crystal with a large van der Waals gap along c. Thus, if the resistivity measurements have been done along c, the system should show insulating behavior, reminiscent of cuprates. Figure 4(c) shows that on further increasing the pressure to $P > P_c'$ the metallicity remains with further widening of the bands and even near closure of the gap between the p states of O, Cl and the d states of Ti. Therefore, this phase transition is induced by structural changes and bandwidth widening [22].

4.2. AFe_2As_2 under pressure

In figure 5, we show the comparison of densities of states calculated based on optimized and experimental lattice structures for $CaFe_2As_2$ in both the AF orthorhombic phase and the paramagnetic 'collapsed' tetragonal phase at low temperature. Figures 5(a) and (b) show a comparison of DOS in the orthorhombic phase. It is found that the DOS are almost the same although the volume and the magnetic moment are both overestimated by DFT calculations within the spin-polarized GGA functional. Figures 5(c) and (d) are the comparison of DOS in the 'collapsed' tetragonal phase and figures 5(e) and (f) the corresponding comparison of pDOS of Fe d states. It is obvious that both DOS and pDOS are almost identical. Peaks coming from Fe d_{xz}/d_{yz} and $d_{x^2-y^2}$ are shifted away from the Fermi level due to the structural change under pressure which avoids the high instability at the Fermi level present in the high-temperature tetragonal phase. Considering the fact that the change of the lattice structure under elevated pressure observed experimentally can be described well by our CP-PAW calculations, in particular the jumps of the volume and the distances of Fe–As at the phase transition which are the two key quantities determining the volume collapse and the electronic properties, respectively (as shown in [49]), we come to the conclusion that our DFT structural optimizations are valid in both low-temperature phases, namely, the AF orthorhombic phase and the 'collapsed' tetragonal phases, except that we have to apply higher pressure than the critical value obtained from experiments to eliminate the overestimated magnetic moment and volume at ambient pressure and to reach the experimental volume conditions. In order to avoid confusion, we renormalized the pressure with respect to the critical value throughout this work.

In figures 6(a) and (b) we present the calculated changes of the volume and magnetization of AFe_2As_2 (A = Ca, Sr, Ba) as a function of pressure. In the case of $CaFe_2As_2$, the volume and the magnetization decrease gradually with increasing pressure and show a discontinuity at the critical pressure, where the system undergoes simultaneously the structural and magnetic phase transitions from an AF orthorhombic phase to a volume 'collapsed' paramagnetic phase. Our results are in very good agreement with experimental data [34] with a volume collapse of $\Delta V^{\text{th}} \approx 4.1\%$, $\Delta V^{\text{exp}} \approx 4\%$.

In figure 6, we also show the predictions for $SrFe_2As_2$ and $BaFe_2As_2$. We find that the structure and the magnetic phase transitions under pressure still occur simultaneously in these two compounds, but the nature of the phases is distinctly different from the $CaFe_2As_2$ case. This has not yet

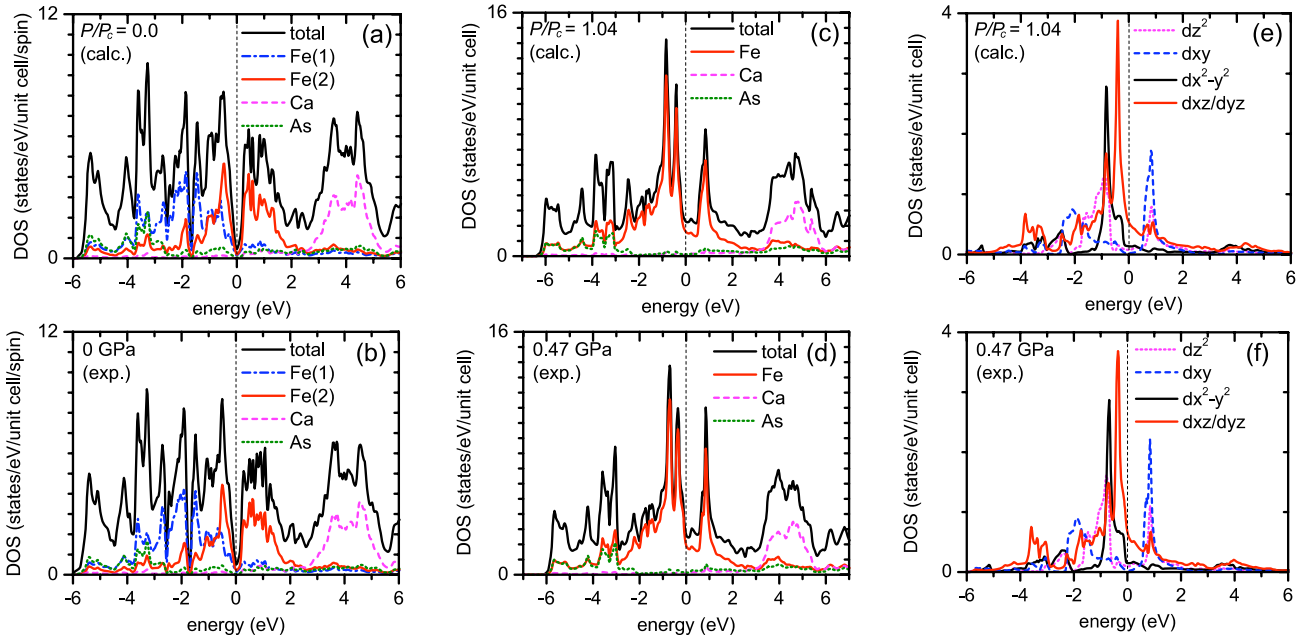

Figure 5. Comparison of DOS for $CaFe_2As_2$ calculated for optimized and experimental lattice structures in both AF orthorhombic phase ((a), (b)) and paramagnetic 'collapsed' tetragonal phase ((c), (d)) at low temperature. A more detailed comparison of the pDOS of Fe d states is shown in (e) and (f).

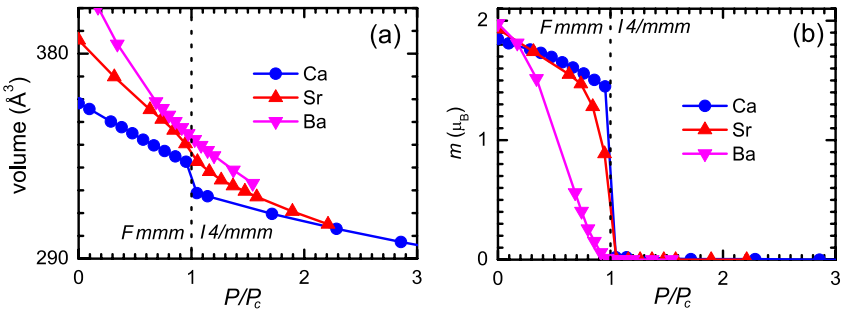

Figure 6. Calculated changes of (a) volume and (b) magnetization of AFe_2As_2 (A = Ca, Sr, Ba) as a function of pressure, normalized to the corresponding critical pressures.

been confirmed experimentally due to the problem of high Sn content [36] in the samples. $SrFe_2As_2$ shows smaller magnetization and volume jumps at the critical pressure compared to $CaFe_2As_2$ while we can hardly detect any discontinuity in $BaFe_2As_2$, which in this respect resembles more closely [50] the parent compound of the iron pnictide superconductors, LaFeAsO.

In summary, by considering *ab initio* Car–Parrinello molecular dynamics calculations, we were able to describe the microscopic details of the pressure-induced phase transitions in TiOCl and the family AFe_2As_2 (A = Ca, Sr, Ba) with very good agreement with experimental observations. The CP-PAW proves to be a reliable and powerful method to describe structural and magnetic changes at the phase transition.

Acknowledgments

We thank the Deutsche Forschungsgemeinschaft for financial support through the TRR/SFB 49 and Emmy Noether programs.

References

[1] Bednorz J G and Mueller K A 1988 *Rev. Mod. Phys.* **60** 585
[2] Kurosaki Y, Shimizu Y, Miyagawa K, Kanoda K and Saito G 2005 *Phys. Rev. Lett.* **95** 177001
[3] Kandpal H C, Opahle I, Zhang Y-Z, Jeschke H O and Valentí R 2009 *Phys. Rev. Lett.* **103** 067004
[4] Fang Z, Solovyev I V, Sawada H and Terakura K 1999 *Phys. Rev.* B **59** 762
[5] Kasinathan D *et al* 2006 *Phys. Rev.* B **74** 195110
[6] Kuneš J, Lukoyanov A V, Anisimov V I, Scalettar R T and Pickett W E 2008 *Nat. Mater.* **7** 198
[7] Austin I G 1962 *Phil. Mag.* **7** 961
McWhan D B and Rice T M 1969 *Phys. Rev. Lett.* **22** 887
[8] Kuntscher C A, Frank S, Pashkin A, Hoinkis M, Klemm M, Sing M, Horn S and Claessen R 2006 *Phys. Rev.* B **74** 184402
[9] Forthaus M K, Taetz T, Moeller A and Abd-Elmeguid M M 2008 *Phys. Rev.* B **77** 165121
[10] Kamihara Y, Watanabe T, Hirano M and Hosono H 2008 *J. Am. Chem. Soc.* **130** 3296
[11] Torikachvili M S, Bud'ko S L, Ni N and Canfield P C 2008 *Phys. Rev. Lett.* **101** 057006

[12] Car R and Parrinello M 1985 *Phys. Rev. Lett.* **55** 2471
[13] Parrinello M and Rahman A 1980 *Phys. Rev. Lett.* **45** 1196
[14] Seidel A, Marianetti C A, Chou F C, Ceder G and Lee P A 2003 *Phys. Rev.* B **67** 020405(R)
[15] Hoinkis M *et al* 2005 *Phys. Rev.* B **72** 125127
[16] Shaz M, van Smaalen S, Palatinus L, Hoinkis M, Klemm M, Horn S and Claessen R 2005 *Phys. Rev.* B **71** 100405(R)
[17] Krimmel A *et al* 2006 *Phys. Rev.* B **73** 172413
[18] Rückamp R, Baier J, Kriener M, Haverkort M W, Lorenz T, Uhrig G S, Jongen L, Müller A, Meyer G and Grüninger M 2005 *Phys. Rev. Lett.* **95** 097203
[19] Abel E T, Matan K, Chou F C, Isaacs E D, Moncton D E, Sinn H, Alatas A and Lee Y S 2007 *Phys. Rev.* B **76** 214304
[20] Sing M, Glawion S, Schlachter M, Scholz M R, Goss K, Heidler J and Claessen R 2009 arXiv:0905.1381
[21] Zhang Y-Z, Foyevtsova K, Jeschke H O, Schmidt M U and Valentí R 2009 arXiv:0905.1276
[22] Zhang Y-Z, Jeschke H O and Valentí R 2008 *Phys. Rev. Lett.* **101** 136406
[23] Blanco-Canosa S, Rivadulla F, Pineiro A, Pardo V, Baldomir D, Khomskii D I, Abd-Elmeguid M M, Lopez-Quintela M A and Rivas J 2009 *Phys. Rev. Lett.* **102** 056406
[24] Kuntscher C A, Pashkin A, Hoffmann H, Frank S, Klemm M, Horn S, Schoenleber A, van Smaalen S and Hanfland M 2008 *Phys. Rev.* B **78** 035106
[25] Huang Q, Qiu Y, Wei Bao, Green M A, Lynn J W, Gasparovic Y C, Wu T, Wu G and Chen X H 2008 *Phys. Rev. Lett.* **101** 257003
[26] Rotter M, Tegel M and Johrendt D 2008 *Phys. Rev.* B **78** 020503(R)
[27] Goldman A I, Argyriou D N, Ouladdiaf B, Chatterji T, Kreyssig A, Nandi S, Ni N, Bud'ko S L, Canfield P C and McQueeney R J 2008 *Phys. Rev.* B **78** 100506(R)
[28] Zhao J, Ratcliff W II, Lynn J W, Chen G F, Luo J L, Wang N L, Hu J and Dai P 2008 *Phys. Rev.* B **78** 140504(R)
[29] Yu W, Aczel A A, Williams T J, Bud'ko S L, Ni N, Canfield P C and Luke G M 2008 arXiv:0811.2554v1
[30] Rotter M, Tegel M and Johrendt D 2008 *Phys. Rev. Lett.* **101** 107006
[31] Sasmal K, Lv B, Lorenz B, Guloy A M, Chen F, Xue Y-Y and Chu C-W 2008 *Phys. Rev. Lett.* **101** 107007
[32] Ahilan K, Ning F L, Imai T, Sefat A S, McGuire M A, Sales B C and Mandrus D 2009 *Phys. Rev.* B **79** 214520
[33] Saha S R, Butch N P, Kirshenbaum K and Paglione J 2009 *Phys. Rev.* B **79** 224519
[34] Kreyssig A *et al* 2008 *Phys. Rev.* B **78** 184517
[35] Goldman A I *et al* 2009 *Phys. Rev.* B **79** 024513
[36] Kumar M, Nicklas M, Jesche A, Caroca-Canales N, Schmitt M, Hanfland M, Kasinathan D, Schwarz U, Rosner H and Geibel C 2008 *Phys. Rev.* B **78** 184516
[37] Lee H, Park E, Park T, Ronning F, Bauer E D and Thompson J D 2009 arXiv:0809.3550v1
[38] Alireza P L, Ko Y T C, Gillett J, Petrone C M, Cole J M, Lonzarich G G and Sebastian S E 2009 *J. Phys.: Condens. Matter* **21** 012208
[39] Colombier E, Bud'ko S L, Ni N and Canfield P C 2009 *Phys. Rev.* B **79** 224518
[40] Kimber S A J *et al* 2009 *Nat. Mater.* **8** 471
[41] Fink J *et al* 2009 *Phys. Rev.* B **79** 155118
[42] Zhang Y-Z, Jeschke H O and Valentí R 2008 *Phys. Rev.* B **78** 205104
[43] Mastrogiuseppe D M, Torio M E, Gazza C J and Dobry A O 2008 arXiv:0812.0542
[44] Mastrogiuseppe D and Dobry A 2009 *Phys. Rev.* B **79** 134430
[45] Pisani L, Valentí R, Montanari B and Harrison N M 2007 *Phys. Rev.* B **76** 235126
[46] Saha-Dasgupta T, Lichtenstein A and Valentí R 2005 *Phys. Rev.* B **71** 153108
[47] Blöchl P E 1994 *Phys. Rev.* B **50** 17953
[48] Mazin I I, Johannes M D, Boeri L, Koepernik K and Singh D J 2008 *Phys. Rev.* B **78** 085104
[49] Zhang Y-Z, Kandpal H C, Opahle I, Jeschke H O and Valentí R 2009 *Phys. Rev.* B **80** 094530
[50] Opahle I, Kandpal H C, Zhang Y, Gros C and Valentí R 2009 *Phys. Rev.* B **79** 024509
[51] Yildirim T 2009 *Phys. Rev. Lett.* **102** 037003
[52] Xie W, Bao M, Zhao Z and Liu B-G 2009 *Phys. Rev.* B **79** 115128
[53] Blaha P *et al* 2001 *WIEN2K, An Augmented Plane Wave + Local Orbitals Program for Calculating Crystal* K Schwarz (ed) Techn. University, Vienna, Austria
[54] Pisani L and Valentí R 2005 *Phys. Rev.* B **71** 180409
[55] Kotliar G 2003 *Science* **302** 67
[56] Kuntscher C A 2008 private communication